Journal of Alloys and Compounds 509 (2011) 4643–4648

Contents lists available at ScienceDirect

Journal of Alloys and Compounds

journal homepage: www.elsevier.com/locate/jallcom

Synthesis and characterization of sol–gel hydroxyapatite coatings deposited on porous NiTi alloys

J.X. Zhang[a,b], R.F. Guan[a], X.P. Zhang[a,*]

[a] School of Materials Science and Engineering, South China University of Technology, Tianhe, Wushan Road 381, Guangzhou 510640, China
[b] Department of Chemistry, Jinan University, Guangzhou 510632, China

ARTICLE INFO

Article history:
Received 26 November 2010
Received in revised form 22 January 2011
Accepted 27 January 2011
Available online 4 February 2011

Keywords:
Porous NiTi alloy
Hydroxyapatite coating
Sol–gel
Ni ion release
Apatite forming ability

ABSTRACT

A hydroxyapatite (HA) coating was deposited onto a porous NiTi alloy via dip-coating using a sol–gel procedure with triethyl phosphite and calcium nitrate as phosphorus and calcium precursors, respectively. Adjusting the concentration and viscosity of the sol as well as changing the spin-coating rotational velocity or dip-coating times, enabled uniform coatings with controllable thickness at the sub-micron scale to be successfully deposited on the external surface and within the pores of the porous NiTi alloy. Cross-sectional SEM analysis and EDS characterization of the HA films show that the coating on the inner surface of the pores is thicker than that on the outer surface. The results of an immersion test in a Tris solution show that the HA coating possesses excellent stability, and the rates of Ni ion release through the HA coatings on the porous NiTi alloys of different porosity ratios in a simulated body fluid decrease markedly compared with the uncoated alloys. There is also a remarkable increase in the apatite forming ability of the HA coated porous NiTi alloy in a calcium containing solution.

1. Introduction

NiTi shape memory alloys are important biomaterials for use in medical devices because of their unique properties, such as shape memory effect, superelasticity and high damping capacity [1,2]. In particular, NiTi shape memory alloys have been widely used in the field of orthopedic surgery [3–6]. In comparison with conventional dense NiTi alloys, the porous NiTi alloy not only keeps the excellent mechanical properties of the bulk NiTi alloys, but also shows some special advantages; for example, the interconnected porous structure may facilitate the transportation of body fluids and further promote bone tissue ingrowth, which enables integration with the surrounding tissue more firmly, leading to the enhancement of interfacial stability. Recently, porous NiTi alloys with controllable pore features and thus tailored mechanical properties can be fabricated [7–9], which may further enhance their applicability for replacement of real bones. Nowadays, it is commonly accepted that the porous NiTi alloys are becoming one of the most suitable and promising biometals for bone repair or replacements [10,11].

However, there is a major concern regarding the biocompatibility of the NiTi alloy due to the high Ni content in the alloy, which may bring about Ni ion release due to in vivo corrosion of the NiTi alloy, regardless of dense or porous. The released Ni ions may be allergenic and toxic when the accumulation of Ni ions reaches a sufficiently high level. In particular for the porous NiTi alloy, the high specific surface area and complicated surface configuration pose a more serious challenge regarding Ni ion release issue than dense NiTi alloy. Therefore, it is imperative to improve the corrosion resistance of NiTi alloys and minimize Ni ion release before considering them safe for clinical biomedical applications.

Surface modification is an effective approach to reduce the corrosion rate of NiTi alloys to an acceptable level. A popular method for surface modification of clinical biomedical materials is to use hydroxyapatite (HA) coating due to their excellent biocompatibility and osteo-conductivity. There are several processes to prepare the HA coatings, namely by physical methods such as plasma spraying and ion-beam-assisted deposition, and by chemical methods such as sol–gel and biomimetic processes. Compared with physical methods, chemical treatment is believed to be more suitable with complex surface morphology such as porous structures. Chemical treatment allows the liquid medium full access to the outer surfaces and inner surfaces at a low temperature which would not influence the superelasticity and other mechanical properties of porous NiTi alloys. In a previous study [12], crystalline HA layers were successfully prepared on porous NiTi alloys by chemical treatment in 32.5% HNO_3 solution followed by boiling in 1.2 M NaOH solution and subsequent immersion in a simulated body fluid (SBF). These coatings resulted in lower Ni ion release and simultaneously enhance bioactivity with micrometer scale particle size of HA on porous NiTi alloys, which unfortunately tended to form cracks owing to particle

* Corresponding author. Tel.: +86 20 2223 6396; fax: +86 20 2223 6393.
E-mail address: mexzhang@scut.edu.cn (X.P. Zhang).

0925-8388/$ – see front matter © 2011 Elsevier B.V. All rights reserved.
doi:10.1016/j.jallcom.2011.01.196

Table 1
Ion concentrations (mM) in SBF and FCS solutions [8,9].

	Na^+	K^+	Mg^{2+}	Ca^{2+}	Cl^-	HPO_4^{2-}	SO_4^{2-}	HCO_3^{2-}
SBF	142.0	5.0	1.5	2.5	148.0	1.0	0.5	4.2
FCS	137.0	4.64	–	3.10	145.0	1.86	–	–

aggregation. As an alternative chemical method, sol–gel deposition possesses a number of advantages, such as better control of the chemical composition of the coating, a reduction in the densification temperature of the ceramic layer, and the controllable thickness of the layer which can be achieved by adjusting the concentration and viscosity of the sol and changing the spin-coating or dip-coating time. The process is also a non-line-of-sight process, so it is anticipated to generate uniform coatings on porous substrate. Thus far, there are many studies about preparation of HA coatings on titanium and its alloys as well as other bulk metals by the sol–gel method, whereas preparation of HA coatings on porous NiTi alloys is not reported.

The present study reports our latest results on the successful preparation of dense and uniform HA coatings on both the outer surface of the porous NiTi alloy and within the pores via a sol–gel route employing triethyl phosphite and calcium nitrate as phosphorus and calcium precursors, respectively. The stability of the coating in tris(hydroxymethyl)aminomethane solution and the rate of Ni ion release from the coated porous NiTi alloys with various porosity ratios in SBF solution as well as the apatite forming ability in a calcification solution (FCS) were investigated.

2. Experimental details

2.1. Preparation of porous NiTi alloy samples and HA coatings

The porous NiTi alloys with tailored pore characteristics and adjustable porosity ratio were fabricated by using a temporary space-holder (NH_4HCO_3) and a conventional sintering method developed by our group [7,9]. In this study, the porous NiTi alloy disc samples of 16 mm in diameter and 2 mm in thickness were prepared by electrical discharge machining. The samples were well polished using a series of SiC sandpapers. Then the samples were ultrasonic cleaned with acetone, ethanol and deionized water, each for 20 min, respectively, and finally dried in air. The procedure for preparation of the sol utilises a recent study [13]. Briefly, triethyl phosphite was diluted in anhydrous ethanol and then a fixed amount of deionized water was added for hydrolysis in a paraffin-sealed glass container under vigorous stirring for 24 h. The molar ratio of the water to phosphite was 4. A stoichiometric amount (Ca/P = 1.67) of 2 M anhydrous ethanol calcium nitrate solution which had been vigorous stirred for 3 h was added drop wise into the hydrolyzed phosphite sol. It was required to retain solution transparency during the entire process of drop mixing. The mixed sol solution was then continuously agitated for additional 24 h and then vapour driven off at 60 °C for 72 h until a viscous liquid was obtained. The rinsed porous NiTi alloy samples/substrates were dipped into the sol with the aid of ultrasonic cleaning for 5 min for excluding gas in the pores. Then the substrates were withdrawn at a speed of 20 mm/min at ambient atmosphere. After each dip coating, the samples were dried at 80 °C to evaporate the residual solvent, followed by annealing in air at 450 °C for 2 h. The dip-coating-drying step was repeated several times to obtain the coating with required thickness and quality.

2.2. Microstructural characterization

The surface and the cross-section of the coated porous NiTi alloy samples, before and after immersion in different solutions used in this study, were examined by a scanning electron microscopy (JSM-T300) and the thickness of the coating was determined accordingly. The phase components were analyzed by an X-ray diffractometer (MSAL-XD2, Cu Kα, 36 kV, 20 mA) at a scanning speed of 2° (2θ)/min, from 20° to 80°.

2.3. Evaluation of the stability of the coatings by immersion test in Tris solution

Tris solution can provide the same pH value as body fluid and does not contain other cationic components except H^+ and other anionic except Cl^-, so it can avoid interference from chemical reaction of other ions. The presence of other ions in Tris solution after an immersion test is due to the dissolved coating. Thus, the Tris immersion test is employed to evaluate the stability of the coatings.

Tris solution was prepared by dissolving tris(hydroxymethyl)aminomethane ($(HOCH_2)_3CNH_2$, AR) in deionized water and adding 1.00 mol/L HCl to adjust pH value to 7.25. The concentration of Tris solution is 0.05 mol/L.

The coated samples were immersed in Tris solution at 37 ± 0.5 °C. Every two days, an amount of 5 mL of immersion solution was taken to measure Ca and P concentrations by an inductive coupled plasma emission spectrometer. The total soaking time was 14 days. After the soaking period, the samples were cleaned and dried in air, and then the surface of the samples was examined by SEM.

2.4. Ni ion release test

After the porous NiTi alloy samples of different pore sizes and porosity ratios were coated with HA, the samples were then immersed in a beaker containing 30 mL of SBF for different periods to evaluate the behavior of Ni ion release from the HA coated porous NiTi alloy samples. The immersion test was conduct in SBF at 37 ± 0.5 °C. For comparison, the porous NiTi alloy samples without coating were also tested in SBF. Table 1 gives the ion concentrations of the as-prepared SBF solution [14]. An amount of 5 mL of immersion solution was taken to measure Ni concentration every 2 days, and meanwhile 5 mL of the fresh SBF solution was added into the beaker to maintain a nearly constant concentration of SBF solution.

2.5. Immersion test in FCS

To evaluate the apatite-forming ability of the HA coated porous NiTi alloy samples in comparison with the uncoated one, a fast calcification solution (FCS) [15] was prepared according to the composition shown in Table 1. The samples were immersed in the FCS at 37 ± 0.5 °C and at pH 7.4. The ratio of volume to exposed area was about 0.25 mL/mm^2, with the FCS refreshed every 2 days. The surface of the samples after the soaking was examined by SEM, and apatite particles (crystals) on the coating were taken out of the substrate by gently scraping and then measured with Fourier transform infrared spectroscopy (FT-IR).

3. Results and discussion

3.1. Coating characteristics

The surface morphology of the coated porous NiTi alloy sample is shown in Fig. 1. Clearly, the outer planar surface is covered by a homogeneous coating and no cracks are found as shown in Fig. 1(a) and (c), and so is the curved surface inside the pores of the porous NiTi alloy, see Fig. 1(d). Fig. 2 presents X-ray diffraction patterns from the outer surface and inside the pores of the coated porous NiTi alloy, and the EDS analysis results are also shown (inserted in Fig. 2). In Fig. 2, the peaks of Ca and P are dominant and the ratio of Ca to P is 1.32, which is lower than that in the original sol with the Ca to P ratio of 1.67. Fig. 3 shows XRD patterns of the coated porous NiTi alloy, where the diffraction peaks of (2 1 1), (1 1 2), (3 0 0), (2 0 2) and (0 0 2) corresponding to the HA phase are clearly seen, besides the peaks of NiTi phase. These results prove that the HA coating with calcium deficiency has formed on the surface of the porous NiTi alloy.

Furthermore, in Fig. 1(c) it can be seen that the surface of the porous NiTi alloy matrix is adhered to by uniform spherical HA particles of submicron size, which may be the expected surface structure condition for promoting bone ingrowth; in Fig. 1(d) it is clear that the HA coating is uniformly deposited on the inner side of the pores, which looks clean and shows no impurities.

Moreover, after six cycles of the dipping-drawing-drying-firing process, the cross-section of the HA coatings on outer and inner surfaces was examined by SEM. The interfacial morphologies are shown in Fig. 1(e) and (f), respectively, where the thickness of the coatings on the outer surface reaches 1–2 μm and 3–4 μm on the inner surface. Clearly, the inner surface coating is thicker than the outer surface one and this is caused by more amount of the sol entering into the pores during the dip-coated process under ultrasonic vibration. The cross-sectional images of the coatings also show that the coating–substrate interface is fully dense with no

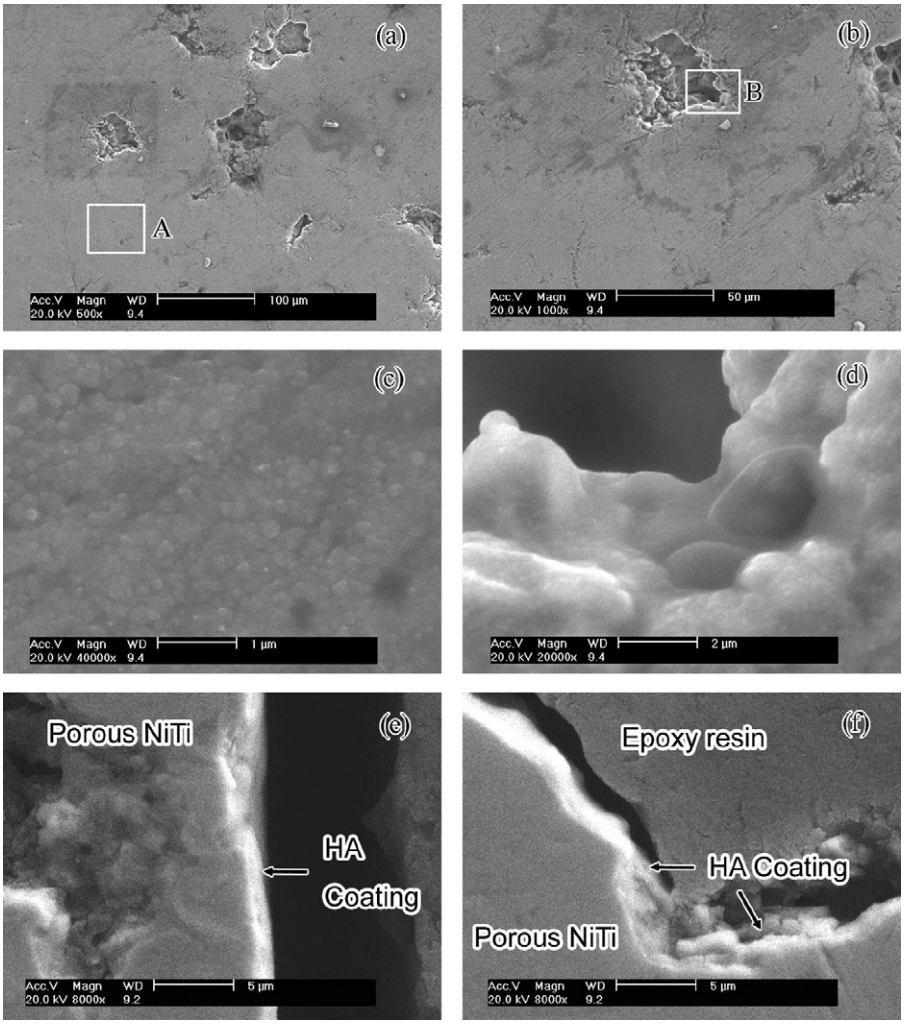

Fig. 1. SEM images of the surface and cross-section of the coated porous NiTi alloy sample: (a) and (b) coated with HA (at a low magnification); (c) high magnification image of the area A in (a); (d) high magnification image of the pore area B in (b); (e) cross-sectional view of the outer surface coating; and (f) cross-sectional view of the inner surface coating.

pores or voids and the bonding between layer and substrate is good.

In addition, it is clear in Fig. 2 that Ti and Ni contents from the outer surface (see Fig. 2(a)) are higher than those corresponding to the inner pore (see Fig. 2(b)) and this means that the inner surface coating is thicker than the outer surface one. These results are consistent with those obtained from the cross-sectional examination shown in Fig. 1(e) and (f).

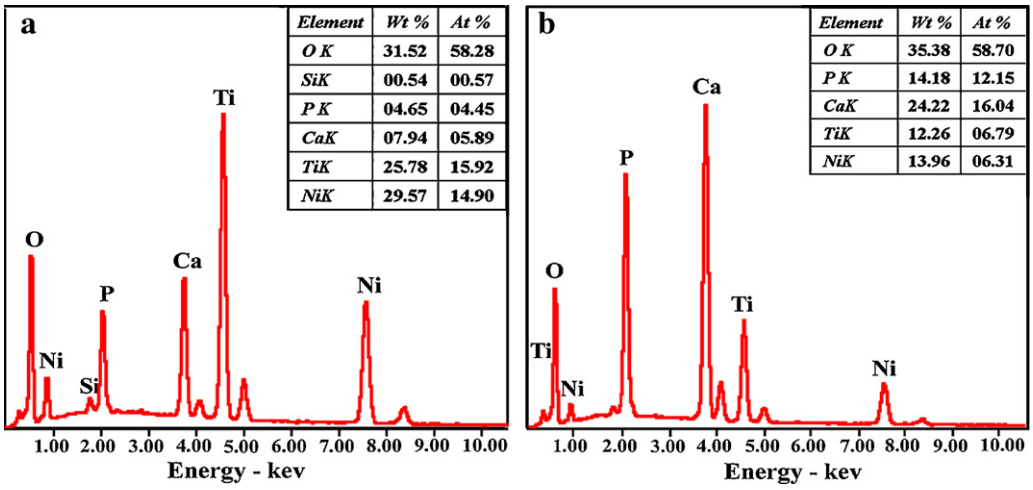

Fig. 2. The EDS analysis results of (a) the outer surface and (b) inside the pores of the coated porous NiTi alloy.

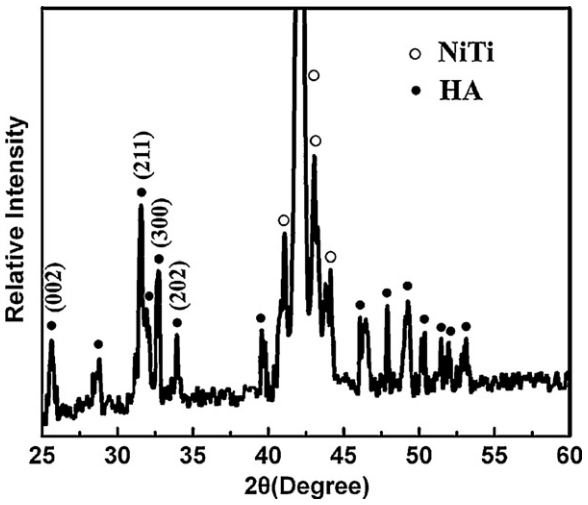

Fig. 3. XRD patterns of the HA coated porous NiTi alloy.

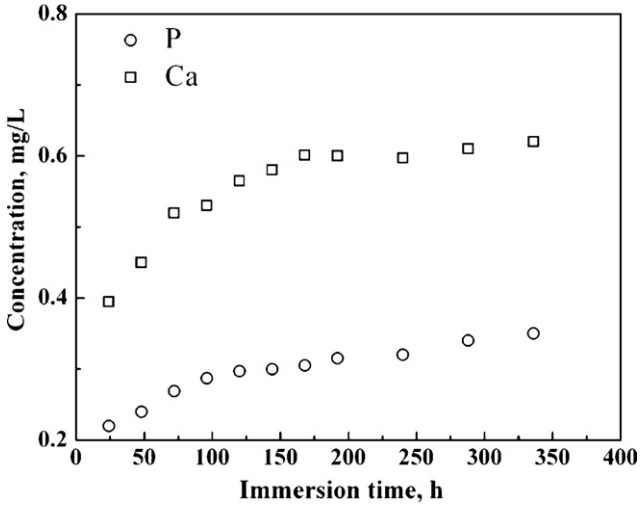

Fig. 5. The Ca and P concentrations in Tris solution versus immersion time.

3.2. Stability of the coatings in Tris solution

The surface morphology of the HA coated porous NiTi alloy after two weeks immersion in Tris solution is shown in Fig. 4. Compared with Fig. 1(a), there is no obvious change in the surface morphology and most of the surface area is covered by smooth and continuous coating. The result shows that the HA coating has good stability in Tris solution. In addition, a small amount of spherical particles appear on the surface, which originate from redeposition of some dissolved HA coatings on the substrate. In the experiment, the sol–gel derived HA coatings on the porous NiTi alloy consist of mainly apatite phase (AP) and amorphous calcium phosphate phase (ACP). Generally, the solubility of calcium phosphate obeys the following rule: the solubility of ACP is greater than that of HA [16]. In immersion test in Tris solution, some amorphous calcium phosphate phases in the coating tend to dissolve in the solution and cause an increase of Ca and P concentrations at the initial stage of immersion, as shown in Fig. 5. Then, with the increase of Ca and P concentrations, the Ca and P ions in the solution may re-deposit on the substrate and reach a precipitation–dissolution equilibrium during the subsequent immersion period. It has been indicated that the re-deposition process of HA a spontaneous reaction from Ca and P ions in solution which may occur as follows [17]: ACP is spontaneously precipitated out of the solution first, and then the ACP is changed into ocatacalcium phosphate (OCP) under the action of the solution, finally OCP hydrolyzed into HA phase. Because these reactions took place on the coating, the product was also attached to the coating. Accordingly, the coating morphology was also affected in the process of conversion of ACP to HA. The conversion of ACP to the transitional product OCP was not an in situ growth process. Thus, with the dissolution of ACP and the growth of OCP, some surface pits appear on the original flat coating due to ACP dissolution and some small particles emerge owing to HA growth eventually.

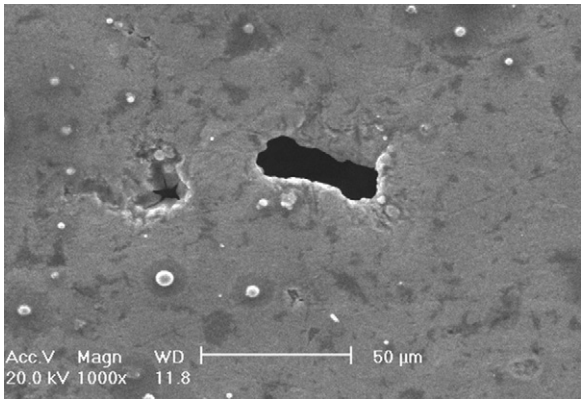

Fig. 4. SEM image of the surface morphology of the coating after two weeks immersion in Tris solution.

3.3. Time dependence of Ni ion release

The rates of Ni ion release from the un-coated and HA coated porous NiTi alloy samples of various porosity ratios in SBF are plotted against time in Fig. 6. Clearly, the rates of Ni ion release from the HA coated samples with the four porosity ratios decrease with immersion time and are much lower than that of the uncoated sample. Furthermore, it is clear that the rate of Ni ion release from the sample with a high porosity ratio is greater than that of the sample with a low porosity ratio. As discussed in the above immersion test in Tris solution, the preferential dissolution of ACP can cause surface pits on the original flat coating, which may produce an exposed surface in direct contact with simulated body fluid if the thickness of the coating is small. The following reaction would occur due to Cl^- adsorption on the exposed surface [18]:

$$Ni + 2Cl - 2e = NiCl_2 \quad (1)$$

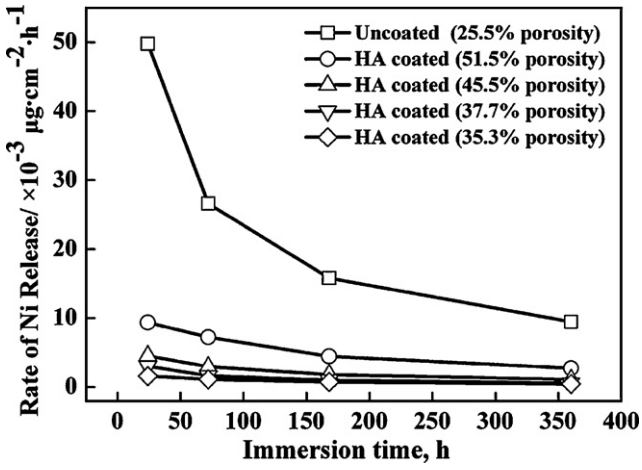

Fig. 6. Change of concentration of Ni ion released from uncoated and HA coated porous NiTi alloy samples in SBF with immersion time.

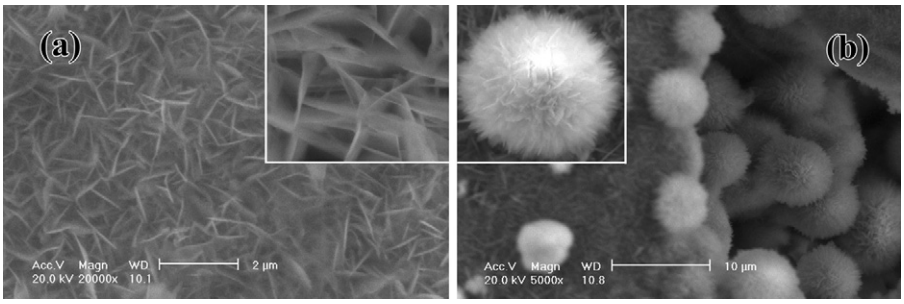

Fig. 7. SEM images of the surface morphology of the HA coated porous NiTi alloy after immersion in SBF for 10 days: (a) the outer surface and (b) the inner surface.

$$Ni + 2H_2O - 2e = NiO + 4H^+ \quad (2)$$

$$NiO + 2Cl^- + 2H^+ = NiCl_2 + H_2O \quad (3)$$

These reactions all act to form localized pitting sites as the anode, and the surrounding HA coated surface which may act as cathode was protected.

For the porous NiTi alloy samples with various porosity ratios, the characteristics of the pores, such as the shape, depth and the number of pores, can directly affect the crystallinity and thickness of the coating during the dip-coating process and the subsequent sintering process. Thus, the possibility of generating pitting corrosion on the surface during the immersion test increases and the rate of Ni ion release also increases with increasing the porosity ratio. Meanwhile, the results in Fig. 6 suggest that the porosity ratio in the range of 35.3–45.5% shows only a slight effect on the rate of Ni ion release at the same immersion time. But for the sample with a porosity ratio of 51.5%, the rate of Ni ion release is much higher.

Moreover, the results in Fig. 6 show that the rate of Ni ion release for all the samples becomes a maximum after immersion for 24 h and then decreases gradually. It is also clear that the dissolution rate of the coating is greater than the redeposition rate of Ca and P in the solution in the early stage of the immersion and it reaches a precipitation–dissolution equilibrium during the subsequent immersion process.

3.4. Apatite-forming ability

Fig. 7 shows SEM images of the surface morphology of the HA coated porous NiTi alloy samples after immersion in FCS for 10 days. In Fig. 7(a), flake-like apatite crystals have formed on the outer surface and some petal-like circular clusters apatite crystals of a few microns in size present on the inner surface as shown in Fig. 7(b).

In the classical Ostwald's nucleation theory [19], the nucleation free energy (ΔG) depends on the supersaturation of solution (S), the net interfacial energy for nucleation (σ), the temperature (T) and the particle surface area (A), and ΔG can be expressed by $\Delta G = -RT\ln S + \sigma A$. This nucleation theory indicates that increasing the solution supersaturation (S) and reducing the net interfacial energy (σ) can induce heterogeneous nucleation. In the present study, the supersaturation in FCS was greatly increased to reduce the nucleation free energy ΔG. The reduction of ΔG induces heterogeneous nucleation on the outer surface and inner surface. Furthermore, the rough surface on the inner surface of the HA coated porous NiTi alloy, as shown in Fig. 1(d), decreases the net interfacial energy (σ) effectively. Therefore, the nucleation rate of apatite phase greatly increased, and accordingly some petal-like circular clusters apatite crystals formed due to flake-like crystals aggregation growth. In contrast to Fig. 7, there is no detectable apatite deposition due to immersion on the uncoated porous NiTi alloy. These results indicate that the HA coated surface is favorable for apatite formation, and this is consistent with the reported studies that oxide layers containing Ca ions would increase the apatite forming ability [20] or an HA coating would definitely favor apatite formation in SBF [21].

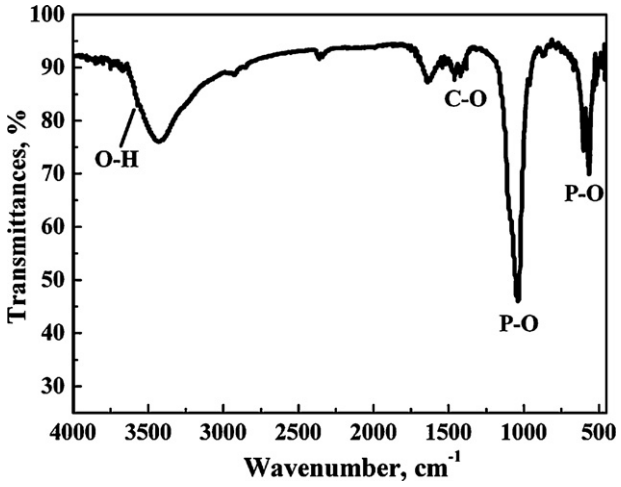

Fig. 8. FT-IR spectra of apatite on HA coatings.

The FT-IR spectra of the apatite crystals on the surface of HA coating are shown in Fig. 8. It is clear that the apatite crystals contain both OH^- and PO_4^{3-} groups. In addition, a CO_3^{2-} vibration band was also been detected due to the dissolution of CO_2 present in the air into the solution, replacing part of the PO_4^{3-} group.

4. Conclusions

(1) A uniform HA coating layer has been deposited on porous NiTi alloys via the sol–gel route. The HA coating, with a thickness at a sub-micron scale, has been formed not only on the surface of the porous NiTi alloy but also inside the pores without blocking them.
(2) The sol–gel derived HA coating shows good stability in Tris solution. The rate of Ni ion release from the HA coated porous NiTi alloys with various porosity ratios in SBF is much smaller compared with the uncoated one.
(3) There is a remarkable increase in the apatite forming ability of the HA coated porous NiTi alloy in FCS and the inner surface of porous NiTi alloy has an increased apatite deposition rate due to the rough surface.

Based on these observations and characterization, it may be concluded that the sol–gel method provides an effective way to produce the HA coating on porous NiTi alloys with the enhanced apatite forming ability beneficial for biomedical applications.

Acknowledgements

This research was supported by the National Natural Science Foundation of China under Grant nos. 50871039 and 50671037, and the Fundamental Research Funds for the Central Universities (No. SCUT-2009ZM0160). Thanks also go to Prof. Michael Swain at the University of Sydney, Australia and Dr. X.T. Sun at South China University of Technology for helpful discussion.

References

[1] K. Dai, Bio-med. Mater. Eng. 6 (1996) 233–240.
[2] A. Kapanen, J. Ilvesaro, A. Danilov, J. Ryhanen, P. Lehenkari, J. Tuukkanen, Biomaterials 23 (2002) 645–650.
[3] V. Brailovski, F. Trochu, Bio-med. Mater. Eng. 6 (1996) 291–298.
[4] F. Mei, X. Ren, W. Wang, Spine 22 (1997) 2083–2088.
[5] J. Musialek, P. Filip, J. Nieslanik, Arch. Orthop. Trauma Surg. 117 (1998) 341–344.
[6] W. Xu, T.G. Frank, G. Stockham, A. Cuschieri, Ann. Biomed. Eng. 27 (1999) 663–669.
[7] Y.P. Zhang, D.S. Li, X.P. Zhang, Scr. Mater. 57 (2007) 1020–1023.
[8] D.S. Li, Y.P. Zhang, G. Eggeler, X.P. Zhang, J. Alloys Compd. 470 (2009) L1–L5.
[9] D.S. Li, Y.P. Zhang, X. Ma, X.P. Zhang, J. Alloys Compd. 474 (2009) L1–L5.
[10] A. Bansiddhi, T.D. Sargeant, S.I. Stupp, D.C. Dunand, Acta Biomater. 4 (2008) 773–782.
[11] B. Bertheville, Biomaterials 27 (2006) 1246–1250.
[12] H.C. Jiang, L.J. Rong, Surf. Coat. Technol. 201 (2006) 1017–1021.
[13] C. Eichenseer, J. Will, M. Rampf, S. Wend, P. Greil, J. Mater. Sci.: Mater. Med. 21 (2010) 131–137.
[14] P. Li, C. Ohtsuki, T. Kokubo, K. Nakanishi, N. Soga, T. Nakamura, T. Yamamuro, J. Appl. Biomater. 4 (1993) 221–229.
[15] H.B. Wen, J.R. Dewijn, Q. Liu, K. Degroot, J. Mater. Sci.: Mater. Med. 8 (1997) 765–770.
[16] J.C. Elliott, Structure and Chemistry of the Apatites and Other Calcium Orthophosphates, Elsevier, Amsterdam, 1994, pp. 4–6.
[17] E.D. Eanes, in: Z. Amjad (Ed.), Amorphous Calcium Phosphate: Thermodynamic and Kinetic Consideration in Calcium Phosphates in Biological and Industrial Systems, Kluwer Academic Publishers, Boston, 1998, pp. 27–30.
[18] X.D. Su, W.C. Hao, T.M. Wang, Chin. J. Mater. Res. 27 (2007) 454–458.
[19] H.M. Kim, Y.J. Kim, S.J. Park, C. Rey, H.M. Lee, M.J. Glimcher, J.S. Ko, Biomaterials 21 (2000) 1129–1134.
[20] T. Hanawa, Mater. Sci. Eng. 267A (1999) 260–266.
[21] H. Wang, N. Eliaz, Z. Xiang, H.P. Hsu, M. Spector, L.W. Hobbs, Biomaterials 27 (2006) 4192–4203.